Hindawi Publishing Corporation
International Journal of Antennas and Propagation
Volume 2010, Article ID 796154, 14 pages
doi:10.1155/2010/796154

Research Article

Design, Analysis, and Measurements of an Antenna Structure for 2.4 GHz Wireless Applications

Constantinos I. Votis,[1] Panos Kostarakis,[1] and Antonis A. Alexandridis[2]

[1] *Physics Department, University of Ioannina, Panepistimioupolis, 45110 Ioannina, Greece*
[2] *Institute of Informatics and Telecommunications, National Centre of Scientific Research "Demokritos", Ag. Paraskeui, 15310 Athens, Greece*

Correspondence should be addressed to Constantinos I. Votis, kvotis@grads.uoi.gr

Received 30 July 2010; Accepted 26 October 2010

Academic Editor: Matteo Pastorino

This paper reports measured results of a multielement antenna implementation, we constructed, that performs at 2.4 GHz ISM band. Particular emphasis was given to the scattering parameters and validation characterization of this antenna structure. The constructed multielement antenna that was studied in both azimuth and elevation planes consists of a number of printed dipoles with integrated baluns. Due to its multielement construction, the proposed antenna structure is suitable for applications that require multielements nature such as MIMO, channel sounder, and digital beamforming.

1. Introduction

Requirements for wider bandwidth capabilities, higher bit rates, and better quality of services are crucial for wireless communication applications. Scientific and engineering community provides a number of novel techniques and methods to meet these requirements. These offer efficient improvements on the throughput of the wireless systems and are usually applied on compatible radiation structures, provided by single or multiple-element antenna architectures. These were further studied in terms of radiation efficiency and performance. Besides, the printed dipole antenna with integrated balun is an attractive type of radiation element that was studied and investigated in previous literature [1–4]. This architecture offers small size, easy, and low-cost antenna implementation. It has omnidirectional radiation characteristics, providing narrowband wireless applications. Several techniques have been introduced to improve the efficiency of this radiation element in terms of frequency bandwidth and antenna gain [5, 6]. Furthermore, this antenna is usually combined with various types of reflector structures in order to improve its directivity and performance efficiency. Microwave theory indicates the impact of the reflector presence and introduces essential observations and principles that confirm the corresponding effects [7, 8]. In each case, scattering parameters and radiation patterns are meaningful on antenna design. The corresponding simulated and experimental results provide an interesting amount of measurements that enhance antenna efficiency and performance.

In addition, the printed dipole antenna with integrated balun and a reflector structure could support multielement antenna configurations because of the compactness and geometry of the whole implementation. The corresponding literature indicates that these multiple-element antenna configurations are mainly used in modern wireless communication applications such as MIMO (Multiple-Input Multiple-Output). These are used on both the transmitter and receiver ends, providing significant enhancement on the capacity of a wireless communication channel. Furthermore, these multiple-element antenna structures support channel sounding and digital beamforming applications along with appropriate signaling techniques.

In fact, these considerations are taken into account in design and implementation of the proposed antenna system. A number of identical printed dipoles and a reflector structure are designed and fabricated for single and multiple antenna elements applications. The geometrical parameters

of them were modified to achieve better performance in the frequency range of 2.4 GHz. This radiation structure is arranged on a wooden base that provides rotation in azimuth and elevation planes and supports radiation pattern adjustments. From these, it seems that the proposed antenna system could be used in a measurement test-bed platform for channel estimation, digital beamforming, and MIMO applications in the frequency range of 2.4 GHz. Single or multiple-element antenna configurations with appropriate RF equipments could be used on transmitting and receiving ends on wireless communication applications. Furthermore, the proposed antenna system provides a number of antenna array topologies due to the reflector nature. This is also an attractive and versatile feature that provides further investigation on wireless channel performance.

For this fact, we are going to use the proposed antenna system as the main part of an RF test-bed platform for both transmitting and receiving purposes. The corresponding results are expected to improve the available channel characterization models and enhance studies on variations of the wireless channel capacity and the correlation of the corresponding subchannels. In addition, the proposed antenna structure provides spatial multiplexing and diversity techniques on MIMO wireless applications because it offers a number of antenna elements on transmitting and receiving ends that are connected with appropriate RF devices. These provide encoding and decoding the main data stream into substreams that are propagated in the wireless channel, simultaneously, providing significant enhancements on the bit rate and quality of service in the current application.

Moreover, using multiple radiation elements in any antenna array configuration on the proposed implementation, we could steer the main beam of the whole radiation structure in a desired direction of transmission or arrival. This corresponds to the digital beamforming method that requires appropriate signaling techniques. Also, a number of similar wireless communication applications are supported by the proposed single-element antenna structure. SISO (Single-Input Single-Output) systems that use only one transmitting and receiving antenna element are the most significant of them.

In any case, the proposed implementation provides a novelty antenna structure for single or multiple ports wireless applications. The compact, easy implemented, and low-cost printed dipole element improves its directivity and efficiency, using the reflector plate structure. The last provides multiple-elements antenna configurations with several geometries and is also arranged on the wooden base structure for better mechanical support, providing rotation on both elevation and azimuth planes, too.

These attractive features of the proposed antenna system are crucial for wireless applications and experimental channel measurements. The performance of the proposed single and multiple-element antenna is investigated by the corresponding simulated and experimental measurements.

In this paper, we propose an antenna implementation for wireless communication applications. In particular, Section 2 describes the corresponding design and implementation of this antenna system. Details on geometry of the printed dipole, reflector plate, and wooden base structure are also provided. The corresponding simulated and experimental results indicate the effect of the reflector and the wooden base structure and are also presented and discussed in Section 3. These correspond to return loss and radiation pattern measurements that allow the validation of the current investigation on antenna performance. The paper concludes in Section 4.

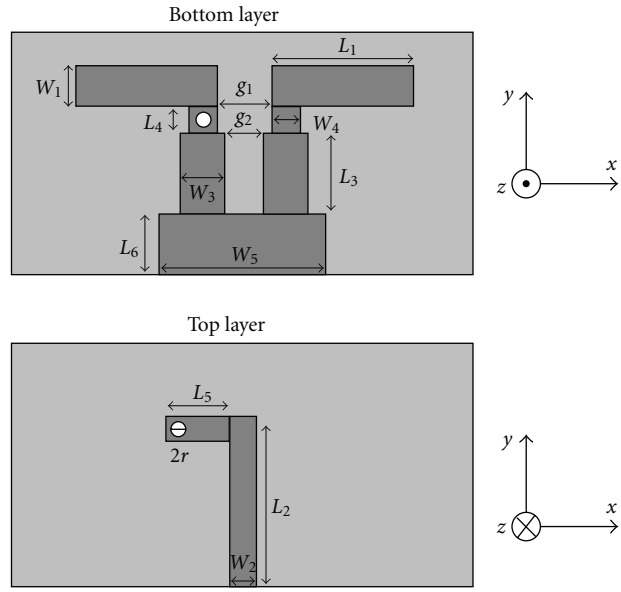

Figure 1: Geometry of printed dipole.

2. Design Process

The construction of the proposed antenna system was carried out into three discrete steps. At first, the printed dipole with integrated balun was designed and implemented to meet the technical requirements for high-quality performance in the frequency range of 2.4 GHz. Figure 1 indicates the geometry of this antenna element at both layers (top and bottom), and the corresponding parameters are included in Table 1. An Fr-4 dielectric substrate with thickness of 1.5 mm and permittivity $\varepsilon_r = 4.4$ was used for the fabrication of this dipole. A representative photo is shown in Figure 2. It also presents the dipole arms (left and right) and gap, the ground plane, the microstrip line, and the balun. In particular, the microstrip line at the top layer feeds the dipole arms, and the integrated balun helps to cancel the current flowing on the outside part of the outer conductor at the coaxial line that is connected to the SMA connector [7].

The same method was used to design and construct a group of identical printed dipoles with integrated baluns in form of a uniform linear antenna array (ULA). In this structure, the distance between the sequential elements approximates the half of the wavelength (λ_0) that corresponds to the frequency range of 2.4 GHz. Figure 3 depicts a representative photo of this multielement antenna configuration.

Table 1: Printed dipole dimensions.

Geometry structure	Parameters—Values
Dipole strip	Length: $L_1 = 20.8$ mm
	Width: $W_1 = 6$ mm
	Gap: $g_1 = 3$ mm
Microstrip balun	Length: $L_2 = 32$ mm
	Length: $L_3 = 16$ mm
	Length: $L_4 = 3$ mm
	Length: $L_5 = 3$ mm
	Width: $W_2 = 3$ mm
	Width: $W_3 = 5$ mm
	Width: $W_4 = 3$ mm
	Gap: $g_2 = 1$ mm
Via radius	$r = 0.375$ mm
Ground plane	Length: $L_6 = 12$ mm
	Width: $W_5 = 17$ mm

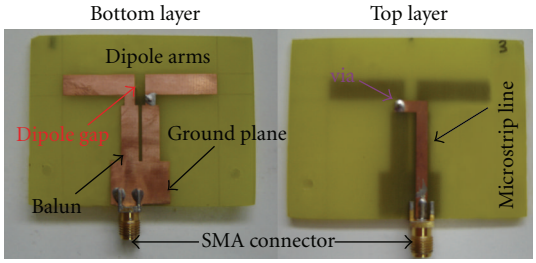

Figure 2: Printed dipole antenna.

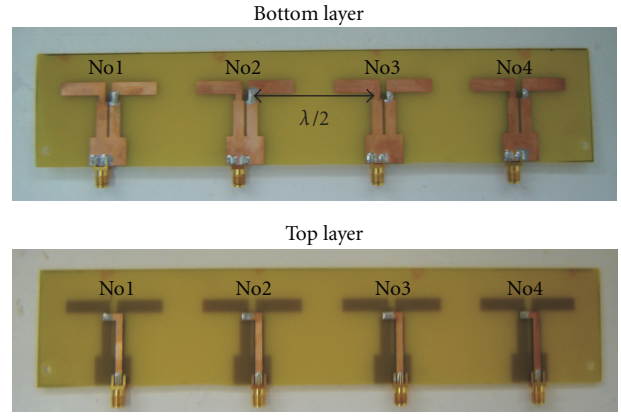

Figure 3: Uniform linear Antenna Array.

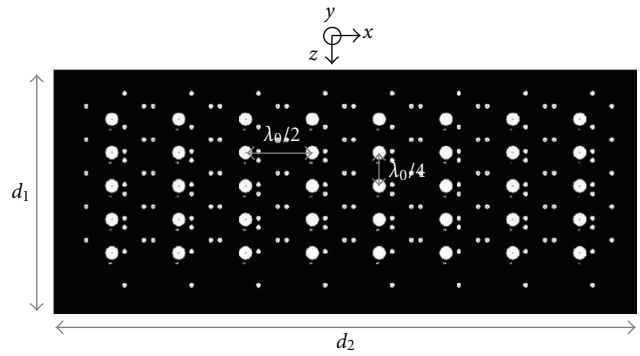

Figure 4: Reflector structure.

This antenna architecture was selected in order to support MIMO and digital beamforming applications. This uniform linear antenna array is a simple and compact structure that provides transmit and receive diversity in wireless applications. As the distance between the sequential radiation elements is equal to $\lambda_0/2$, the RF signals that correspond to the elements of the antenna array are quite uncorrelated. From this consideration, it is convenient that as the wireless channel changes, the signal strength and the phase of these RF signals are varied, quite independently. This observation is very important for capacity enhancements in wireless communication systems [9].

In single or multiple-element case, the proposed antenna configuration is equipped with a reflector plate. The design and implementation of this structure are included in the second step of the antenna system implementation. In particular, the radiation elements are proposed to be arranged on the reflector plate, vertically. For this, a leaf of aluminum plate with 6 mm thickness was used to construct the reflector structure. Figure 4 depicts the reflector geometry.

The corresponding dimensions are $d_1 = 300$ mm and $d_2 = 900$ mm. This reflector architecture provides printed dipole arrangements in several locations. A defined number of holes with two different dimensions have been made on the leaf of aluminum, appropriately. The radius of these holes is 6 mm and 1 mm, respectively. At each wider hole, the SMA connector of the printed dipole may be adapted. Two of the smaller holes that are closed to dipole's location are used to provide its vertical setup on the reflector structure. To obtain this vertical setup, two bases of Plexiglas are also used for each printed dipole. Figures 5 and 6 depict the printed dipole and the uniform linear dipole array on the reflector plate, respectively. This architecture provides the vertical setup of the printed dipoles, avoiding declinations on antenna performance because the dimensions of these bases are quite small and the relative permittivity of this material approximates to 2.6. Furthermore, as the distance between each pair of sequential wide holes is $\lambda_0/2$ for x-axis and $\lambda_0/4$ for z-axis orientation, this reflector structure provides multielement antenna implementations with several topologies.

In Figures 5 and 6, the parameter h represents the distance between the dipole axis and the reflector plate. In the proposed antenna system, this parameter is equal to 34 mm and approximates the quarter of the wavelength ($\lambda_4 = \lambda_0/4$) in the frequency range of 2.4 GHz. Microwave and antenna theory indicates that as the parameter h remains quite less than λ_4, the radiation pattern of the antenna element does not introduce side lobes. It only provides a main lobe [8]. In order to avoid side lobes and declinations on radiation characteristics of the antenna elements in the proposed system, the parameter h was defined to approximate the value of λ_4.

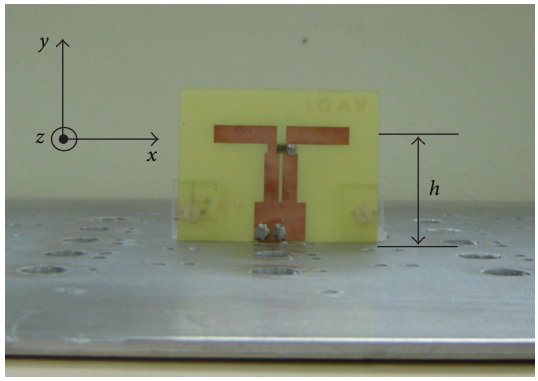

Figure 5: Printed dipole antenna on reflector plate.

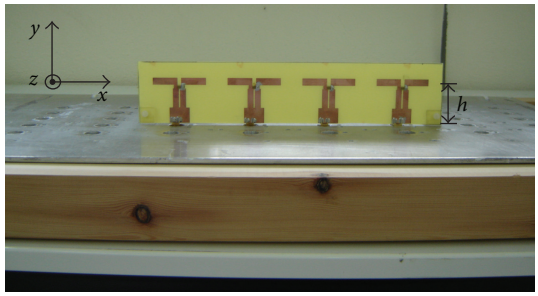

Figure 6: Uniform Linear antenna array on reflector plate.

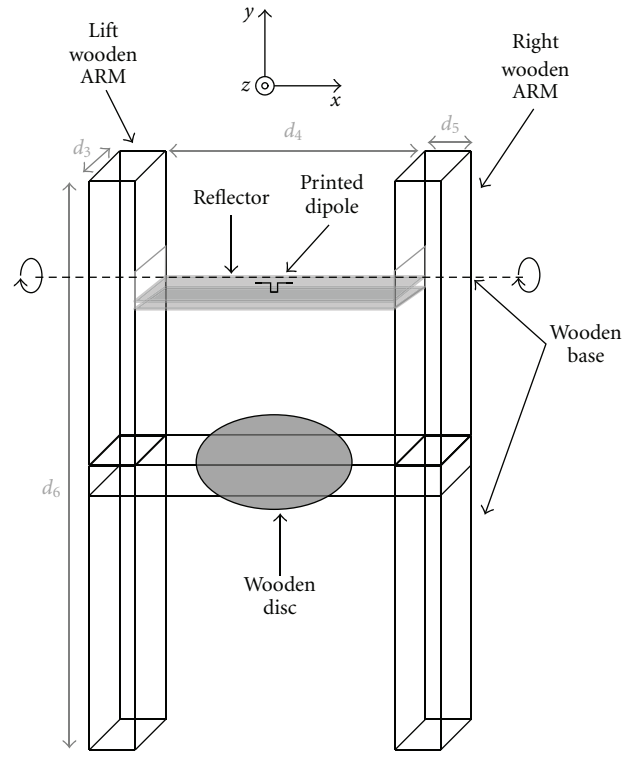

Figure 7: Schematic of the proposed antenna configuration.

Table 2: Geometry of wooden base.

Geometry	Value
d_3	70 mm
d_4	940 mm
d_5	50 mm
d_6	1810 mm

On this investigation, we studied the single element and the four-element uniform linear antenna array performance. The form of the reflector structure provides forty available locations of the printed dipole element. The uniform linear antenna array could be adapted on one of the ten available locations, appropriately. In any case, two orientations are also provided. In particular, the dipole axis will be aligned to x or z axis, and the proposed antenna system could support polarization diversity techniques.

To complete the implementation of the proposed antenna positioning structure, we design and construct a wooden base. The printed dipole elements and the reflector plate of the antenna system are adapted on a wooden base, appropriately. Figure 7 shows a schematic of the proposed implemented wooden base configuration. In this figure, the wooden disc provides rotation adjustments in azimuth plane, as well as the reflector plate on which the printed dipoles are arranged supports rotation adjustments in elevation plane. Table 2 also includes the corresponding geometrical parameters of this wooden base structure.

As mentioned above, the proposed wooden base architecture provides radiation pattern adjustments on both the elevation and azimuth planes. Using dry wood material for this antenna positioning structure, any degradation on the antenna performance is neglected. The relative permittivity of the dry wood material approximates the value of 2 as the RF signal frequency is close to 2.4 GHz. Moreover, this type of wood provides easy and compact implementation on the proposed positioning structure. The design and fabrication process took place on our laboratory, and the engineering staff is familiar with these constructions, using suitable tools and methods. From these considerations, it is obvious that the proposed wooden positioning structure offers rotation adjustments, mechanical stability, easy and low-cost implementation without eliminating the performance efficiency of the radiation elements.

These design considerations have been introduced to fabricate the proposed antenna configuration. Its performance is studied and investigated by a course of detail-simulated and experimental measurements. Next section includes this investigation and the corresponding results.

3. Results and Discussion

In this wooden positioning antenna structure, the scattering parameters and radiation characteristics of the printed dipole antennas are studied and investigated. As mentioned above, the proposed antenna system consists of a reflector plate, a wooden structure, and a number of printed dipole antennas. In this investigation, we studied the impact of the

reflector and wooden structures on the radiation elements performance.

For this, the $S11$ scattering parameter of the printed dipole antenna was simulated over the frequency bandwidth, ranging from 1 GHz to 5 GHz, using a suitable time domain method. In particular, two different circumstances are investigated. The first corresponds to the case that the printed dipole does not neighbor with the reflector plate and the wooden base. The second case introduces the presence of the reflector plate in the defined distance from the dipole axis (h) such as that was depicted by Figure 5, above. Besides, this parameter was measured, using a vector network analyzer. The simulated and experimental results are included in Figures 8(a) and 8(b), respectively.

From these figures, it is obvious that the presence of the reflector plate yields mainly to resonance point shifts. This fact is introduced by the change in the value of frequency that the magnitude of $S11$ parameter of the printed dipole antenna is minimized. In particular, simulated results indicate that the resonance point, at the frequency range of 2.4 GHz, is shifted from 2.49 GHz to 2.36 GHz. Besides, using the value of -10 dB in the magnitude of $S11$ for resonance bandwidth definition, this parameter has a constant value that approximates to 0.4 GHz. On the other hand, the experimental results are in quite good agreement with the simulated measurements. In these curves, the resonance point at the frequency range of 2.4 GHz is also affected by the reflector. In particular, the corresponding value changes from 2.44 GHz to 2.33 GHz, as the printed dipole antenna is arranged on the reflector plate. In each case, the corresponding resonance bandwidths are quite equal, approximating to 0.5 GHz.

From these considerations, it is obvious that the impact of the reflector plate on the magnitude of $S11$ parameter of the dipole structure is provided by quite limited frequency shifting. As this parameter corresponds to the return loss value of the antenna, it seems that the dipole performs efficiently at constant frequency range, approximating the value of 2.4 GHz. This ensures that the amount of energy that is reflected at dipole and feed coaxial line interface remains quite constant and negligible in the frequency range of 2.4 GHz, where the corresponding bandwidth approximates to 0.5 GHz.

Moreover, simulated and experimental results introduce a second resonance point at the frequency range of 4 GHz. The reflector structure affects the magnitude of $S11$ values at this frequency range. A disagreement on the form of this impact is indicated by the simulated and experimental curves, above. In any case, this resonance point is not related with the dipole performance at the frequency range of 2.4 GHz. It seems that the SMA connector and coaxial line in the printed dipole architecture provides this second resonance.

These considerations are related to the single-element antenna design. In order to expand this study on multielement antenna performance, we investigate the magnitude of $S11$ on each of the four dipoles as are arranged on the uniform linear antenna array (ULA) of Figure 3. At first, Figure 9(a) depicts the simulated results that correspond to each of the elements at the ULA array. Besides, the green curve presents the magnitude of $S11$ for the single element case. Moreover, Figure 9(b) includes the corresponding experimental measurements. From these curves, it seems that the performance of each printed dipole is not affected by the presence of the adjacent and identical radiation elements.

More precisely, these elements have the same resonance points, and the corresponding resonance bandwidths are quite identical, too. Mainly from experimental results, it is obvious that the form of each dipole-element curve declines from that which corresponds to single-element case. At the first resonance point, the minimum value of the magnitude of $S11$ parameter approximates to -28 dB for each dipole element in ULA array. Instead, this parameter has a value of -42 dB for single dipole case. Besides, the magnitude of $S11$ range is quite limited for each of the elements in ULA topology at the first resonance bandwidth. In any case, these declinations correspond to quite limited effects on each antenna element performance because of the identical and adjacent dipoles presence.

For further analysis, Figures 10(a) and 10(b) show the magnitude of $S11$ parameter of the single printed dipole and each of the radiation elements in ULA in case of reflector presence.

These simulated and experimental results indicate that the presence of the reflector structure affects the magnitude of $S11$ parameter curves of the printed dipole antenna in both the single and the multiple-element configurations. As mentioned above, the impact of the reflector structure on dipole performance provides frequency point shifting that approximates to 0.12 GHz at the frequency range of 2.4 GHz. This effect is also presented in each dipole element curve that is arranged on ULA topology. In addition, limited declinations between these dipole curves are presented at the first resonance point because of the adjacent elements presence. Generally, each of these radiation elements on the reflector structure has a resonance bandwidth of 0.5 GHz at the frequency range of interest. Based on this fact, it is obvious that the proposed radiation system could support single and multiple-element antenna configurations for narrowband wireless communication applications at the frequency range of 2.4 GHz.

Another important issue on printed dipole performance corresponds to the radiation characteristics and how these are affected by the reflector structure. This impact was studied by measuring the radiation pattern of the printed dipole at the single and multiple-element antenna configurations. In particular, Figure 11 includes the radiation patterns of the printed dipole antenna with and without the reflector's presence on both the E and H planes at 2.44 GHz. As the resonance point of the dipole is shifted from 2.44 GHz to 2.33 GHz by the reflector structure, Figure 12 depicts the radiation patterns of this single element antenna configuration at these two frequency values. The corresponding experimental radiation diagrams are included in Figures 13 and 14, respectively. These are defined by an appropriate amount of experimental measurements in a an RF anechoic chamber, using a calibrated measuring system at the Institute

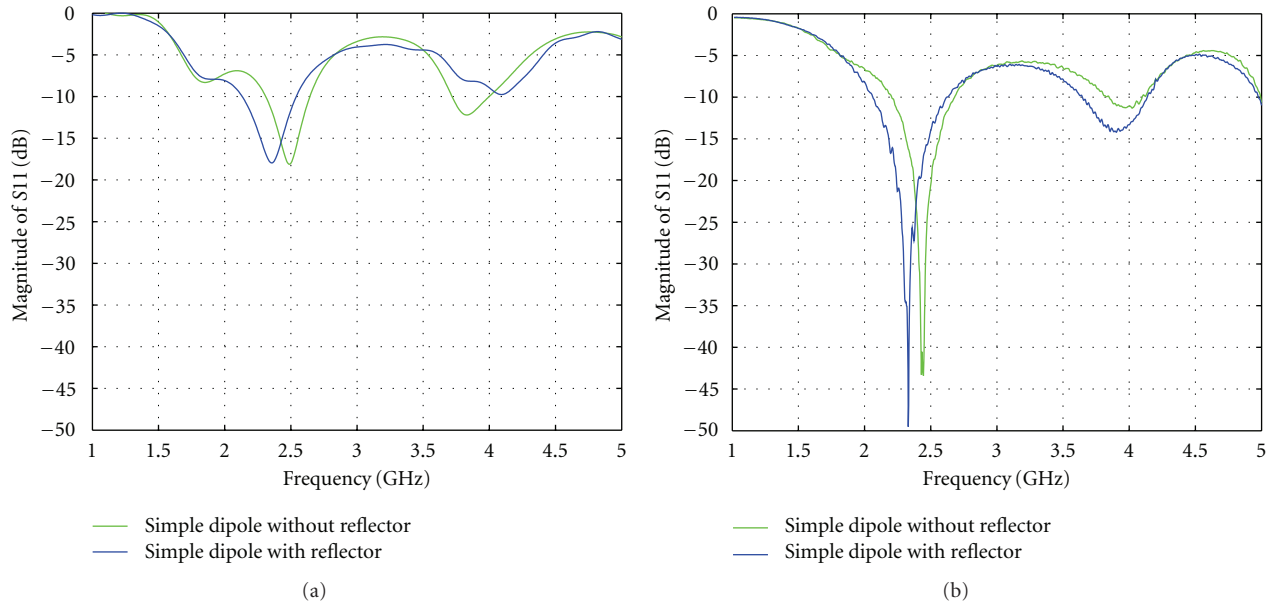

Figure 8: S11 parameter of dipole structure with and without reflector: (a) simulated and (b) measured.

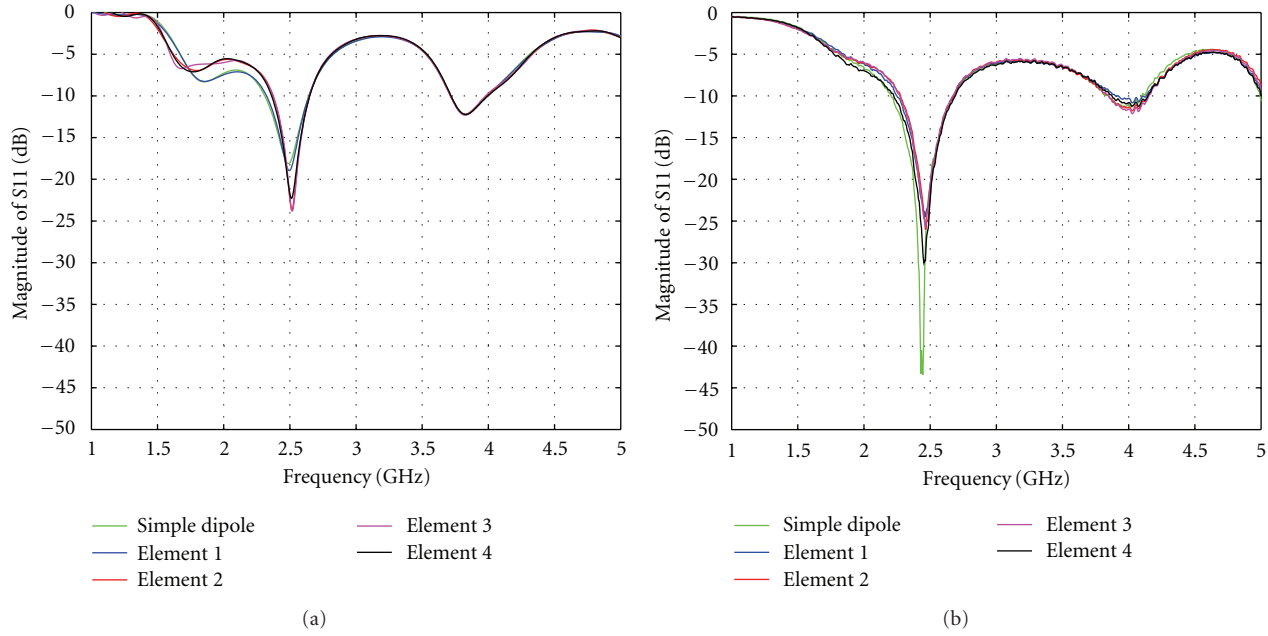

Figure 9: Magnitude of S11 parameter on single dipole and elements on ULA array structures without reflector: (a) simulated and (b) measured.

of Informatics and Telecommunications in National Centre for Scientific Research "DEMOKRITOS." Figure 15 shows a representative photo of these experimental measurements.

At first, Figures 11 and 13 indicate the impact of the reflector structure on the radiation characteristic of the printed dipole antenna. The simulated radiation diagrams are in good agreement with the corresponding experimental measurements. In fact, at H-plane the antenna gain increases and approximates to 6.5 dBi. This observation indicates that the forward radiation field strength is enhanced. Antenna theory and image principles agree with these considerations, too. Furthermore, it is convenient that for this antenna arrangement (dipole on the reflector plate) the number of lobes remains constant (one) [7, 8]. In Figures 12 and 14, the corresponding results indicate that there are no differences in radiation characteristics of the printed dipole with the reflector's presence for these two defined frequencies that approximates to 2.33 GHz and 2.44 GHz, respectively. Based on both

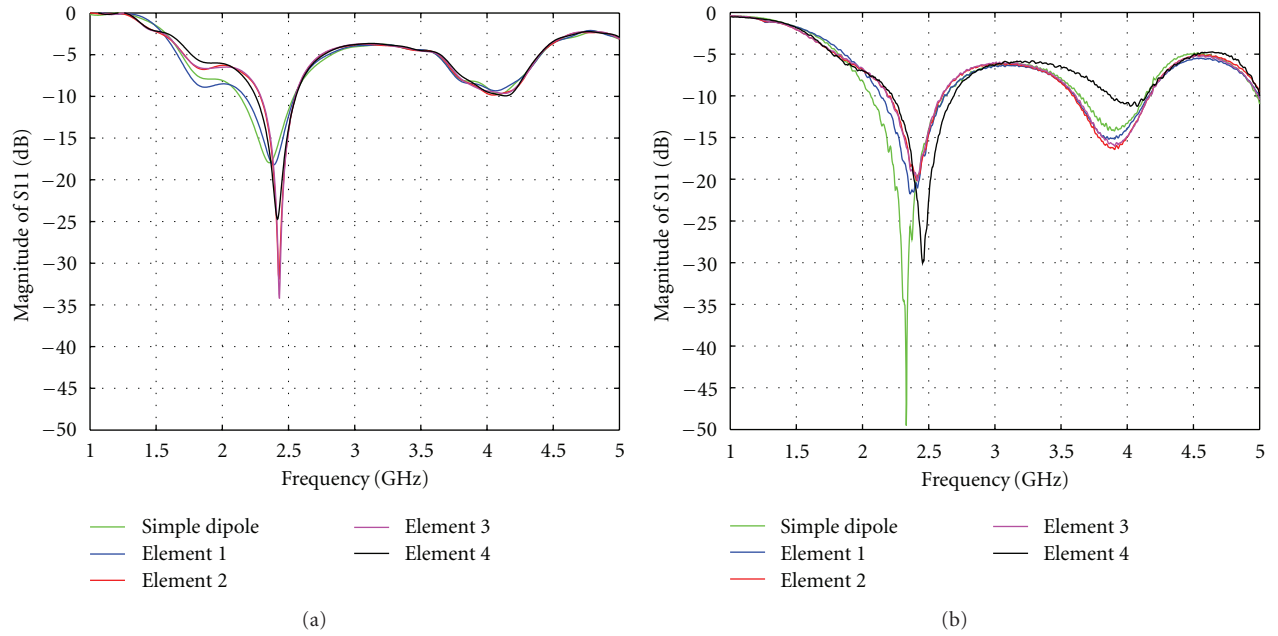

Figure 10: Magnitude of S11 parameter in single dipole and elements on ULA array structures with reflector: (a) simulated and (b) measured.

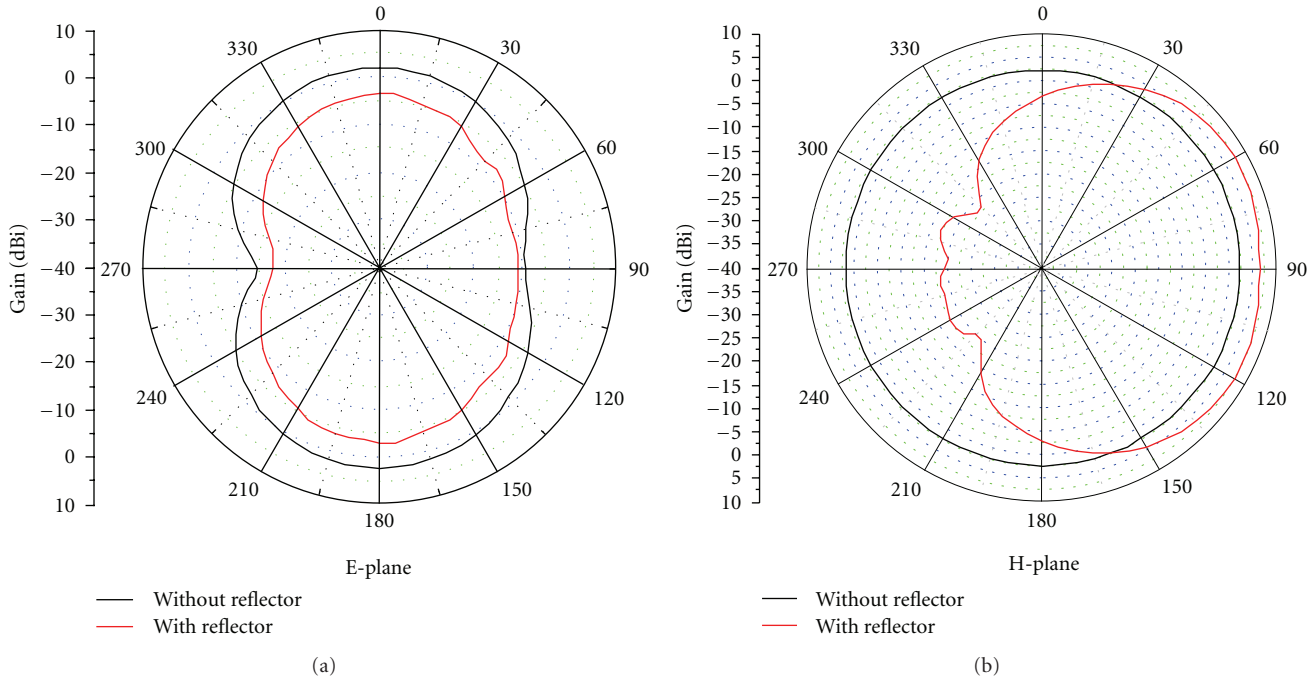

Figure 11: Simulated radiation diagrams of dipole with and without reflector at 2.44 GHz.

simulated and experimental results, it is obvious that the reflector plate improves the directivity of the single element antenna, offering high antenna gain in defined direction. This increased directivity is crucial for wireless system efficiency as the single-dipole antenna steers the main beam at specific direction.

For analysis on multiple-element antenna performance, Figure 16 depicts the simulated radiation pattern of the single dipole and the second element dipole on ULA array. The corresponding experimental results are included in Figure 17. In each case, the single element and four-element antenna performs without the reflector plate at 2.44 GHz.

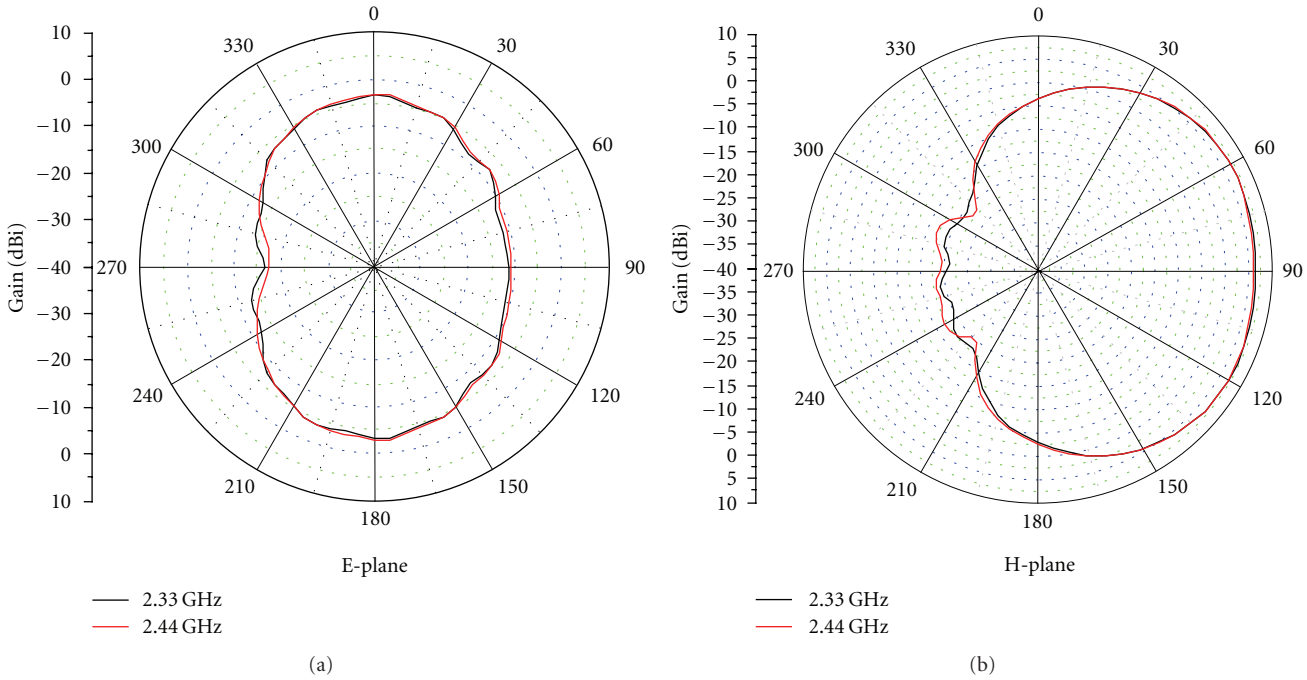

Figure 12: Simulated radiation diagrams of dipole on reflector plate at 2.44 GHz and 2.33 GHz.

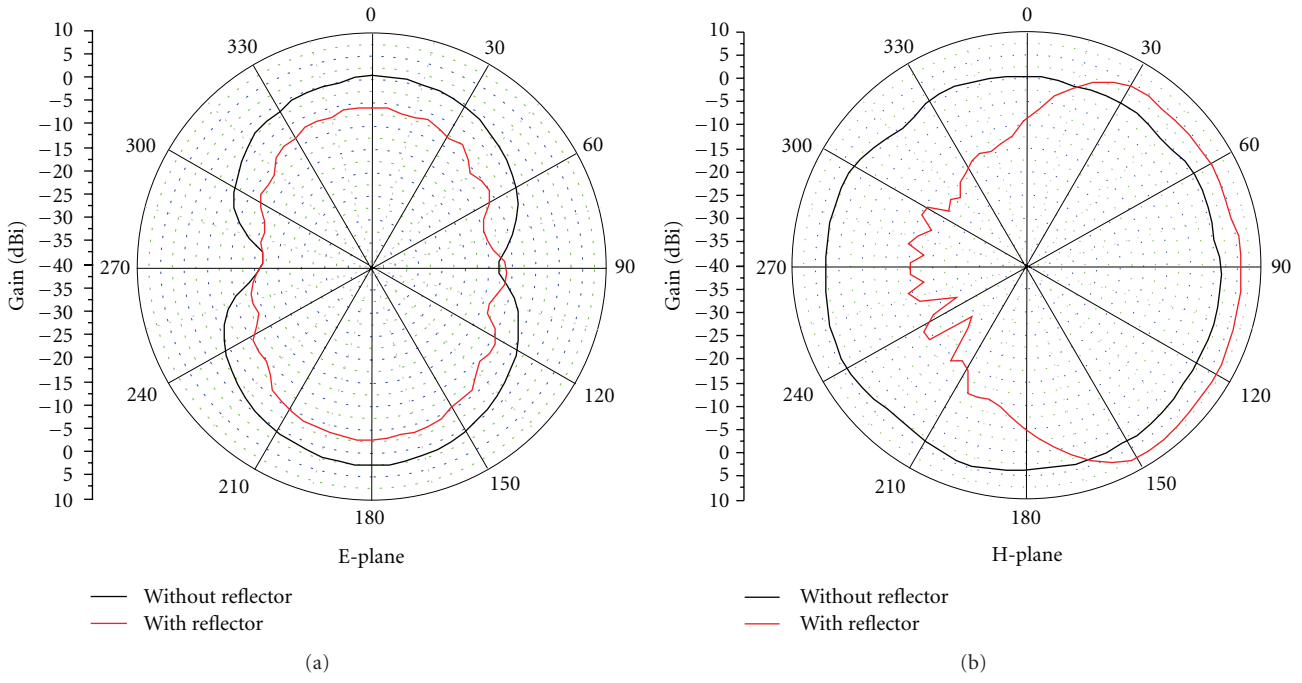

Figure 13: Experimental radiation diagrams of dipole with and without reflector at 2.44 GHz.

From these results, it seems that the printed dipole and the element 2 on the ULA array have the same radiation characteristics on both E and H plane. This consideration indicates that the radiation patterns of each of the four dipoles at the ULA array are not affected by the presence of the adjacent elements. Single or multiple printed dipole antenna configurations have the same radiation characteristics. The last observation is meaningful for multiple-element antenna performance and the corresponding wireless applications.

Furthermore, the impact of the reflector structure on the ULA array was also investigated. For this purpose, Figures 18(a) and 18(b) show the simulated radiation pattern of the second element at the ULA array. These figures include the diagrams on E-plane and xy-plane at 2.33 GHz and 2.44 GHz

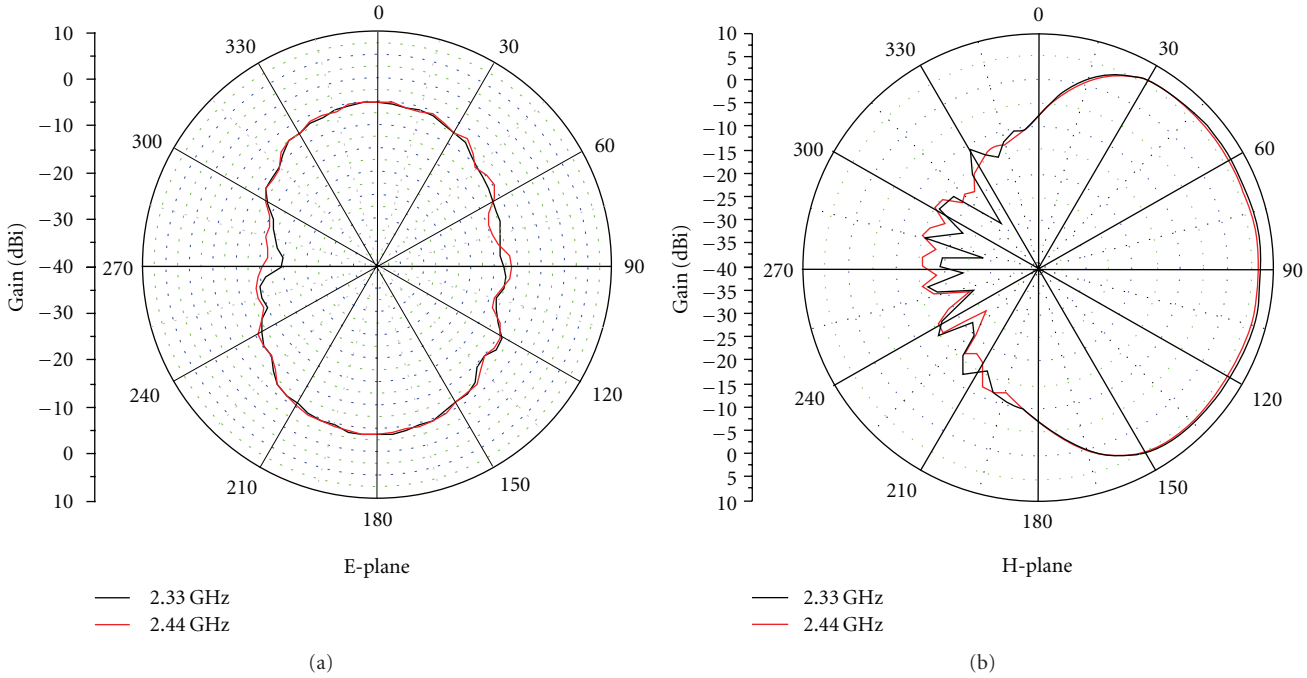

Figure 14: Experimental radiation diagrams of dipole on reflector plate at 2.44 GHz and 2.33 GHz.

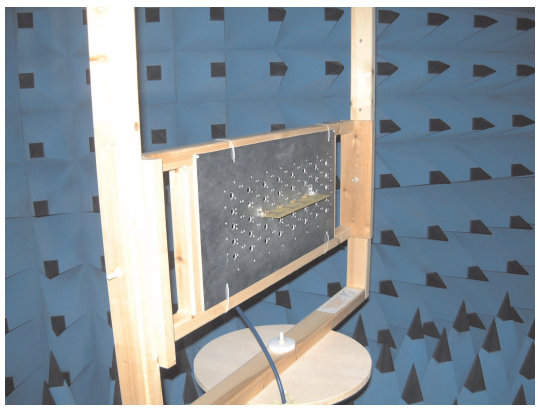

Figure 15: ULA array on reflector plate and wooden positioning structure in RF anechoic chamber.

in case that the ULA array is arranged on the reflector plate. In particular, Figure 18(b) indicates the radiation efficiency of the element 2 in the ULA array at the third plane. The corresponding experimental results are included in Figures 19(a) and 19(b), respectively.

From these radiation patterns, it is obvious that the simulated results are in agreement with the corresponding experimental. Both of them indicate that the element 2 on the reflector plate introduces high direction. This increased value of directivity approximates the corresponding directivity that the single dipole introduces in case of the reflector's presence.

The analysis above corresponds to the reflector structure impact on the single or multiple-element antenna performance. As mentioned in previous section, the reflector plate is arranged on the wooden base, in order to implement the proposed antenna structure. For this, an appropriate analysis on wood effects at antenna performance took place. At first, the magnitude of $S11$ parameter of the printed dipole structure was measured in two different cases, with and without the presence of the wooden base. Figures 20(a) and 20(b) depict the corresponding simulated and experimental results, respectively.

From these curves, it seems that the simulated results indicate no effect on the single printed dipole performance by the wooden base's presence. Instead, the corresponding experimental measurements introduce a quite small increment on the magnitude of $S11$ parameter value at the frequency range of the first resonance point. This disagreement has no importance because of the logarithmic scale on the particular scale. In fact, the difference between these minimum values corresponds to quite negligible difference on the amount of the reflected energy in matching interface between dipole's microstrip line and coaxial line.

For multiple-element antenna configuration, the measurements above were done with the ULA array and the wooden base. In particular, the corresponding simulated and experimental curves for the elements at the ULA array and the single dipole on the wooden base are depicted in Figures 21(a) and 21(b), respectively.

Both simulated and experimental results in these figures above indicate that the impact of the wooden base on the magnitude of $S11$ parameter of the elements at the

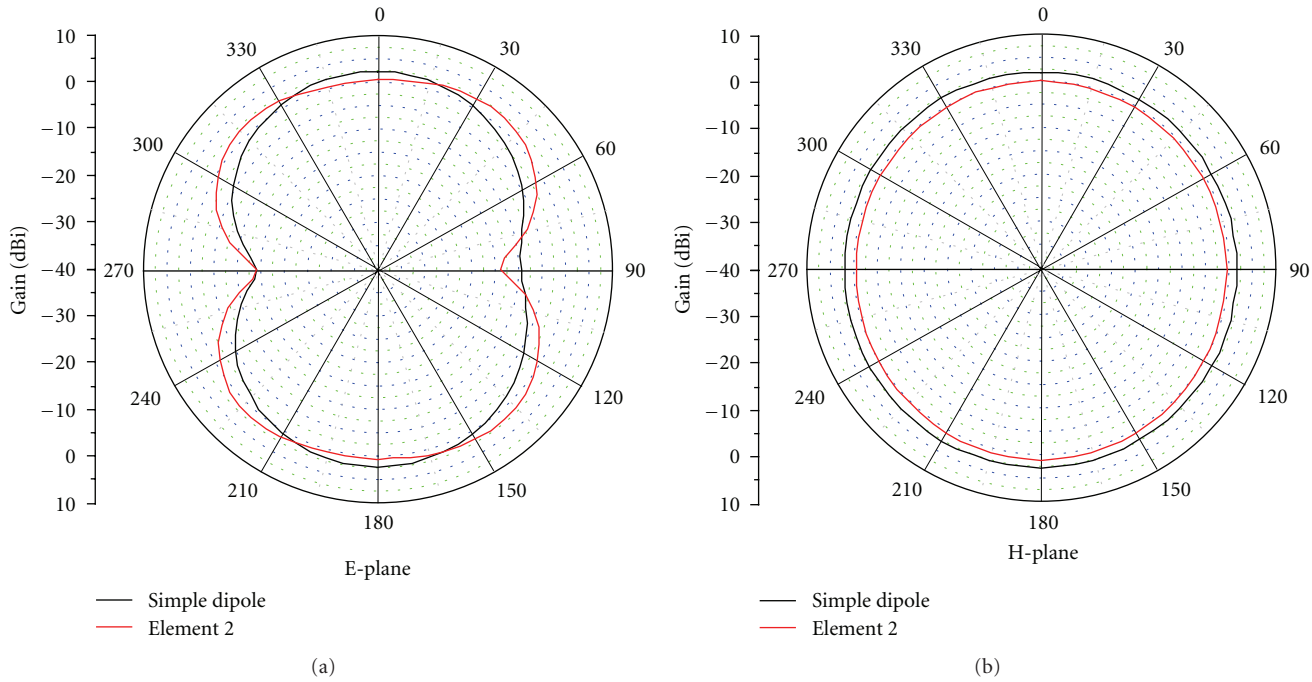

Figure 16: Simulated radiation diagrams of single and element 2 dipoles without reflector plate at 2.44 GHz.

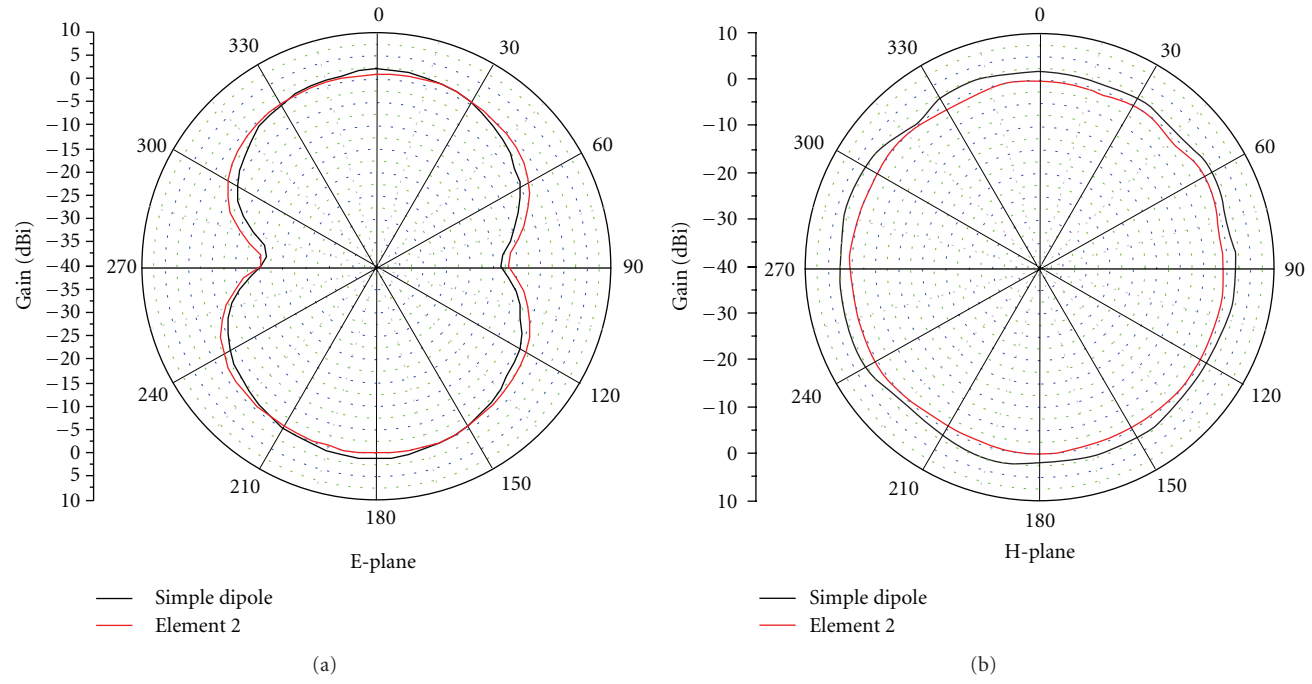

Figure 17: Experimental radiation diagrams of single and element 2 dipoles without reflector plate at 2.44 GHz.

ULA array is quite negligible, in each case. In single or multiple-element antenna configurations, there is no effect on the return loss measurements by the wooden base's presence.

Further investigation on impact of the wooden base in the printed dipole radiation patterns produces an amount of simulated and experimental results. Figure 22 shows a schematic diagram of the corresponding geometry, and Figures 23(a) and 23(b) depict the simulated and experimental radiation patterns on E-plane, respectively.

Both simulated and experimental curves present the gain of the dipole in E-plane for two different cases, with and

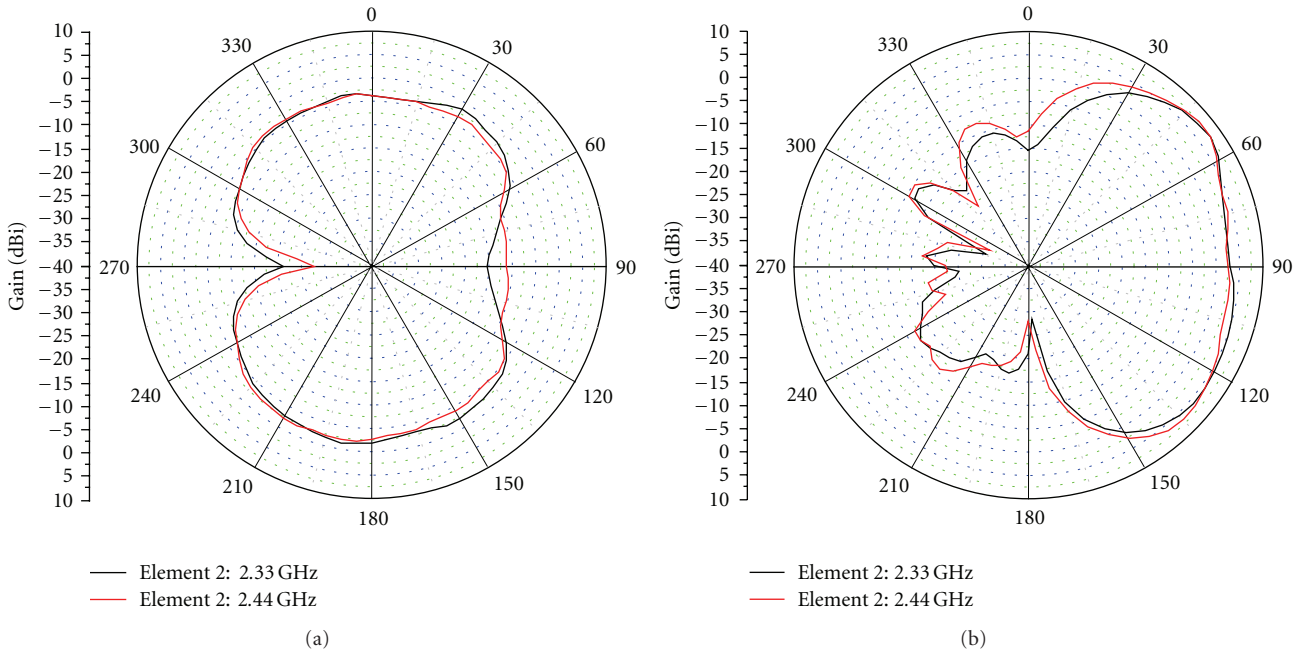

Figure 18: Simulated radiation diagrams of element 2 dipole on reflector plate at 2.33 GHz and 2.44 GHz: (a) E-plane and (b) xy-plane.

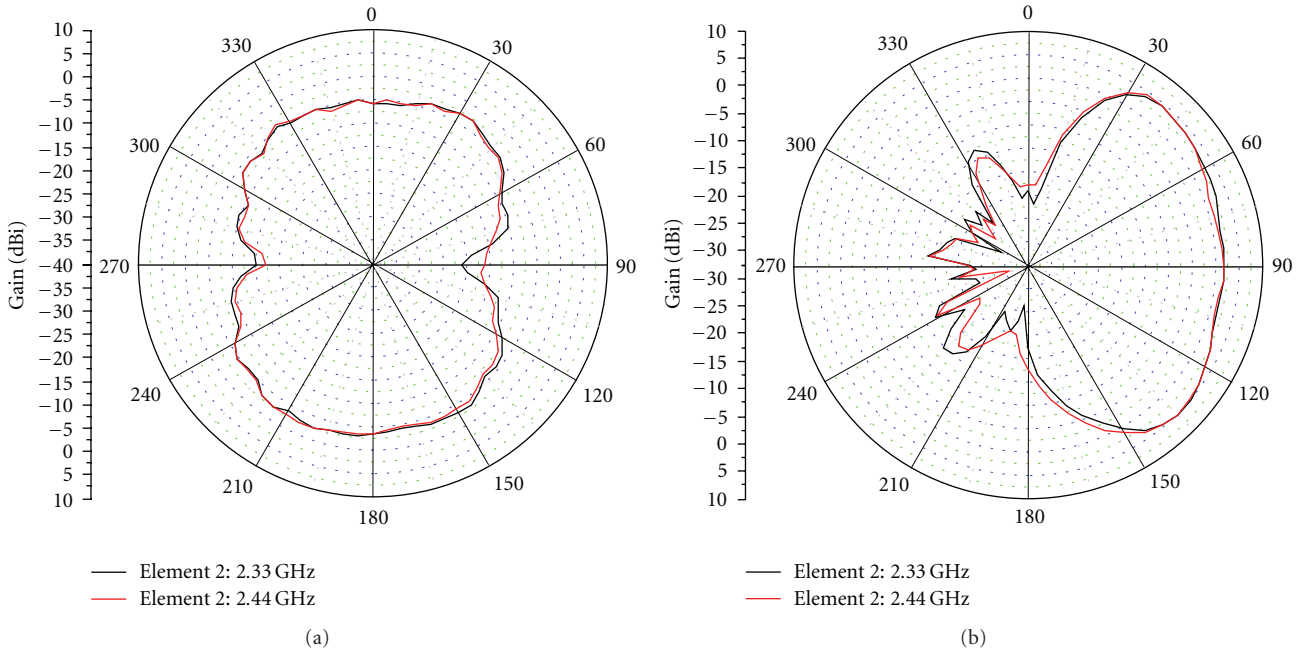

Figure 19: Experimental radiation diagrams of element 2 dipole on reflector plate at 2.33 GHz and 2.44 GHz. (a) E-plane (b) xy-plane.

without the wooden base's presence. From these results, it is realized that the presence of wood affects the radiation pattern of printed dipole and provides small variations on the antenna gain. This observation is crucial in directions where this element radiates, efficiently. For this purpose, the printed dipole orientation is optimized in the proposed antenna implementation. In particular, the printed dipole has to be arranged on the wooden positioning structure, so that its axis is oriented vertical to the wooden arms at the same plane. The dipole axis orientation has to be aligned on x-axis, only. This solution ensures that the quite small variations on the antenna gain of the printed dipole are introduced only in the nulls of its radiation pattern. In order to change the antenna radiation characteristics, mechanical azimuth and elevation adjustments of the proposed positioning structure could be provided.

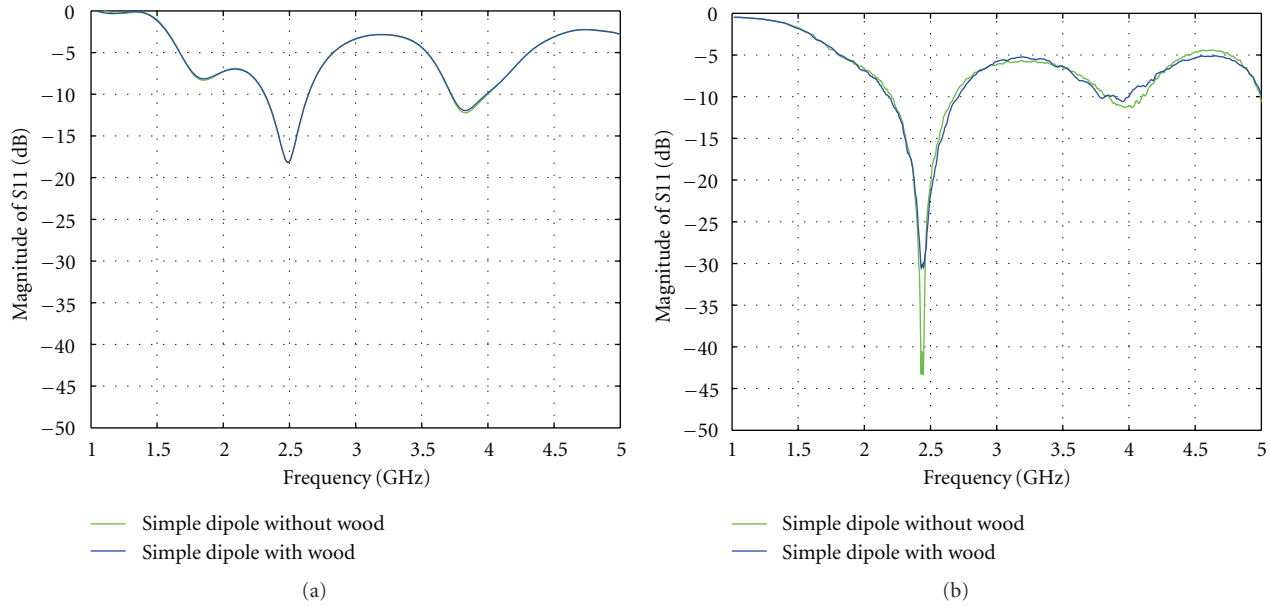

Figure 20: Magnitude of $S11$ parameter of single dipole structure without wooden base and with wooden base: (a) simulated and (b) measured.

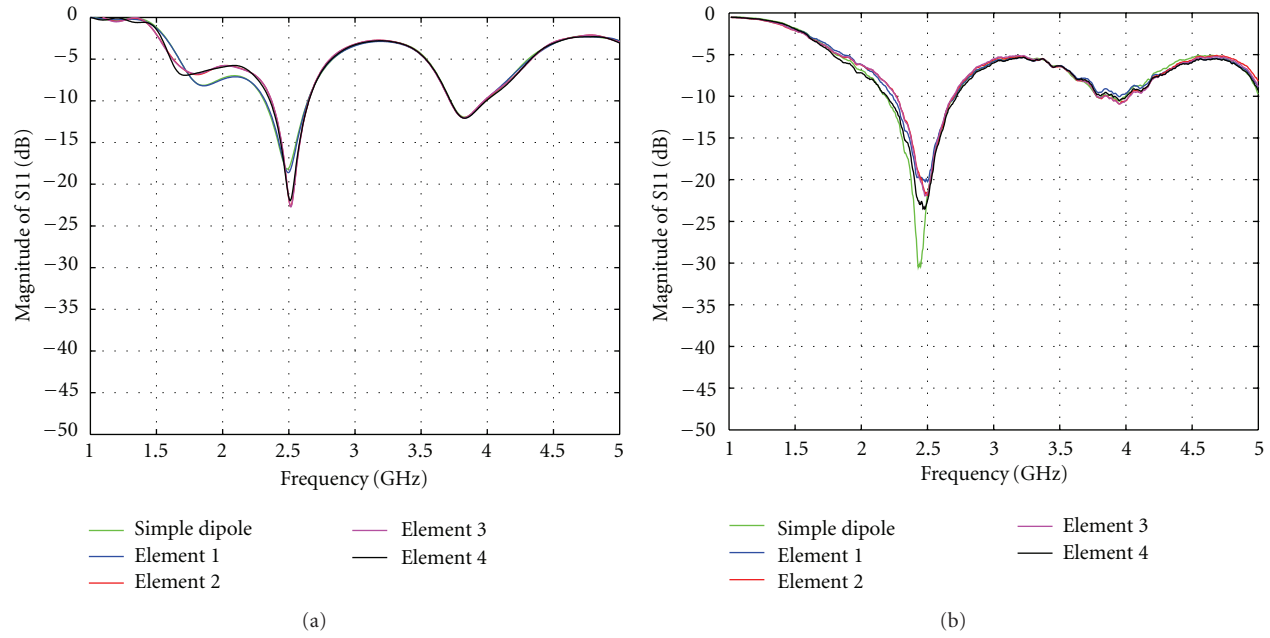

Figure 21: Magnitude of $S11$ parameter in single dipole and elements on ULA array structures with wooden base: (a) simulated and (b) measured.

4. Conclusion

The proposed implementation represents a narrowband antenna configuration for wireless applications at the frequency range of 2.4 GHz. The radiation element is realized by a compact printed dipole with integrated balun. The reflector plate and the wooden base provide antenna's performance. The effect of them on scattering parameters and radiation pattern of the dipole are studied and investigated for single and multiple-element antenna configurations. Simulated and experimental measurements on the magnitude of $S11$ parameter of the printed dipole indicate the impact of the reflector and the wooden base structure. The first yields to resonance point shifting from 2.44 GHz to 2.33 GHz, but the corresponding resonance bandwidth remains constant and equals to 0.5 GHz. It also improves directivity in the radiation pattern of the dipole. The corresponding antenna gain is achieved to approximate the value of 6.5 dBi. Instead, the

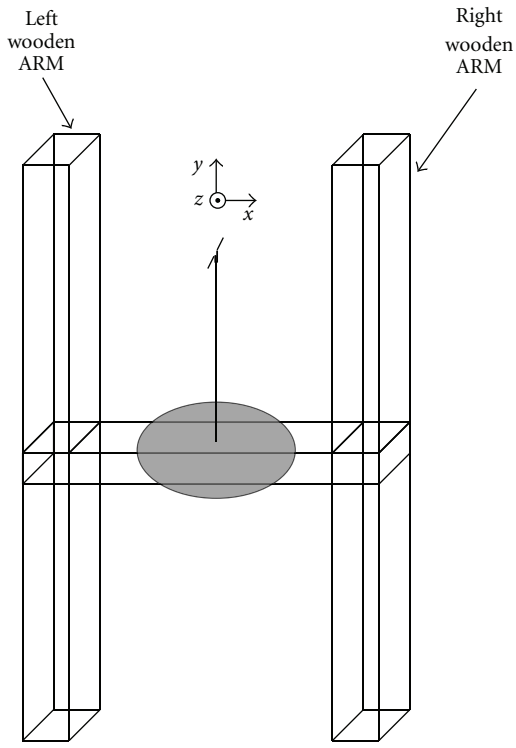

Figure 22: Schematic of investigated antenna configuration.

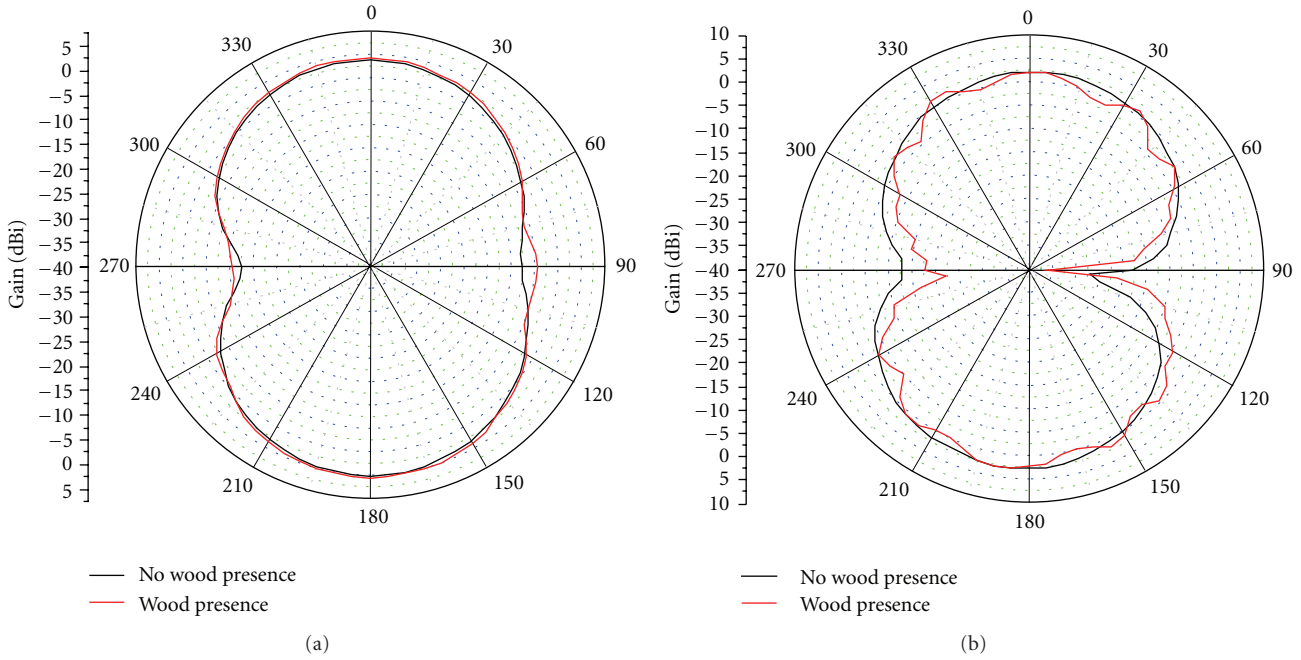

Figure 23: Radiation pattern of dipole with and without wooden base in E-plane: (a) simulated and (b) measured.

wooden base does not affect the return loss of the antenna, but it also provides small variations on the radiation pattern. The proposed wooden positioning structure introduces an optimized arrangement of the printed dipole on the reflector plate and the wooden base in order to ensure high directivity and attractive performance. These observations are crucial for wireless test-bed laboratory applications and communication systems.

Acknowledgments

This research project (PENED) is cofinanced by E.U.-European Social Fund (80%) and the Greek Ministry of Development-GSRT (20%).

References

[1] B. Edward and D. Rees, "A broadband printed dipole with integrated balun," *Microwave Journal*, vol. 30, no. 5, pp. 339–344, 1987.

[2] C. Votis, V. Christofilakis, and P. Kostarakis, "Geometry aspects and experimental results of a printed dipole antenna," *International Journal of Communications, Network and System Sciences*, vol. 3, pp. 97–100, 2010.

[3] G. S. Hilton, C. J. Railton, G. J. Ball, A. L. Hume, and M. Dean, "Finite-difference time-domain analysis of a printed dipole antenna," in *Proceedings of the 9th International Conference on Antennas and Propagation*, pp. 72–75, Eindhoven , The Netherlands, April 1995.

[4] Z. Fan, L. Ran, and K. Chen, "Printed dipole antenna designed with microstrip balun on v-shaped ground plane," in *Progress In Electromagnetics Research Symposium*, pp. 23–26, Hangzhou, China, 2005.

[5] B. G. Duffley, G. A. Morin, M. Mikavica, and Y. M. M. Antar, "A wide-band printed double-sided dipole array," *IEEE Transactions on Antennas and Propagation*, vol. 52, no. 2, pp. 628–631, 2004.

[6] M. C. Bailey, "Broad-band half-wave dipole," *IEEE Transactions on Antennas and Propagation*, vol. 32, no. 4, pp. 410–412, 1984.

[7] D. M. Pozar, *Microwave Engineering*, Wiley, New York, NY, USA, 1998.

[8] C. A. Balanis, *Antenna Theory Analysis and design*, Wiley, New York, NY, USA, 1997.

[9] J. H. Winters, "On the capacity of radio communications systems with diversity in a Rayleigh fading environment," *IEEE Journal on Selected Areas in Communications*, vol. 5, no. 5, pp. 871–878, 1987.